http://journal.uir.ac.id/index.php/JGEET

E-ISSN : 2541-5794
P-ISSN : 2503-216X

Journal of Geoscience,
Engineering, Environment, and Technology
Vol 11 No 2 2026

RESEARCH ARTICLE

Can Liquefaction Be Repeated? An Electrical Resistivity Study at South Palu, Indonesia

Soni Satiawan[1,*], Donar Saragih[2], Dhani Ahmad Hadad[1]

[1] *Geophysical Enginnering Program, Universitas Pertamina, Jakarta Selatan, Indonesia*
[2] *PT. Abhinaya Mappindo Bumitala, Bekasi, West Java, Indonesia*

* Corresponding author : soni.satiawan@universitaspertamina.ac.id
Tel.: +62 812-1950-1075
Received: Nov 13, 2025; Accepted: May 18, 2026.
DOI: 10.25299/jgeet.2026.11.02.25558

Abstract

The recurrence of liquefaction remains a significant concern, prompting a resistivity study in South Palu to investigate subsurface condition associated with this phenomenon. A total of eight lines 2D resistivity lines with dipole-dipole configuration and 10m electrode spacing were acquired in the South Palu subdistrict, covering a cumulative length of 1470m. All stages of data processing and modelling were conducted using a regularized inversion algorithm implemented in the Phyton-based ResIPy software. The inversion results revealed three distinct resistivity layers, low-resistivity ranging from 4.1 – 78.5 ohm.m, interpreted as low permeability a sandy shale or clay rich soil with saturated clay layer extending to a depth of approximately 10m, an underlying high-resistivity layer ranging from 78.6 - 201.4 ohm.m, interpreted as a saturated sand or gravel layer with ± 10m of thickness and associated as a good aquifer and the deep layer at ±20 m depth with highest resistivity (> 200 ohm.m) which is interpreted as compacted sand or hard soil and acted as the base soil in this study area. The evidence of sand intrusion features, upward – moderate to high resistivity intrusions, potentially associated with liquefaction events, were observed in six of resistivity sections. These are indicated by the upward penetration of moderate to high-resistivity value through the low-resistivity layer, towards the surface. Additionally, the recurrence of liquefaction is still conceivable since the existence of ±10m of layer-2 which is interpreted as the most potential liquefiable layer and the thickness of low resistivity of layer-1 and in study area, particularly if subjected to strong earthquake motion.

Keywords: Recurrence, Liquefaction, high-resistivity intrusion, ResIPy

1. Introduction

(Anggorowati & Qodri, 2026)(Ishihara et al., 1990; Kramer, 1996; Tuttle et al., 2019; Anggorowati & Qodri, 2026)The major earthquake in September 2018 at Donggala as epicenter location caused extensive damage to the surrounding Palu city (±32 km from Donggala), primarily due to the triggered liquefaction in several areas and led to significant casualties. The earthquake was the result of active fault zones (Palu – Koro) at shallow depths which are prevalence crossing the Sulawesi Island (Yusran et al., 2020). Liquefaction is a phenomenon where soil loses its strength due to the loss of contact between soil particles and an increase of water saturation within the rock's pores (Ishihara et al., 1990; Kramer, 1996; Tuttle et al., 2019; Anggorowati & Qodri, 2026). The loss of contact between soil particles is often caused by a very large shear force and earthquake being a primary source of such force (Kramer, 1996). As a result, the rock's strength decreases, causing it to behave more like a liquid, which can significantly impact surface infrastructure (Anggorowati & Qodri, 2026).

(Bastola & Acharya, 2016; Tohari et al., 2011; Widyaningrum Risna, 2012) Liquefaction susceptibility is influenced by numerous factors, of which geological and compositional criteria were primarily considered in this study. As a phenomenon restricted to saturated soils, liquefaction occurs within a limited range of geological environments characterized by young, loosely deposited sediment, and exhibiting uniform grain size and sorting. Such conditions are frequently observed in fluvial, colluvial and alluvial settings, which are highly susceptible to liquefaction as seen on Figure 1. Furthermore, given the saturation requirements, groundwater depth plays a significant role, with liquefaction susceptibility increasing in areas where the water table is located within a few meters of the surface (Bastola & Acharya, 2016; Tohari et al., 2011; Widyaningrum Risna, 2012).

Palu garnered global attention following the 2018 earthquake, not merely for the earthquake itself but rather for the tsunami and liquefaction it induced. The liquefaction occurred had been predicted by the researcher (Widyaningrum Risna, 2012) since all the criteria of liquefaction susceptibility could be met in Palu city including young deposit with good sortation (Sukamto RAB., 1973), shallow groundwater depth (Widyaningrum Risna, 2012), and located in alluvial geological environment (Sukamto RAB., 1973). Given Palu City's location within an earthquake-prone area (Soehaimi et al., 2018b) (Soehaimi et al., 2018a) evidenced by its seismicity history (Soehaimi et al., 2018a) and the significant liquefaction observed following the 2018 earthquake, a crucial factor to prioritize in any reconstruction efforts is mitigating the risk of future liquefaction events, both at previously affected sites and in other susceptible areas. Therefore, conducting a comprehensive study to map both the recurrence potential and spatial susceptibility of liquefaction in Palu city's is crucial.

South Palu sub-district was chosen as focused study area, with coordinates 119°52'34.10" - 119°52'8.40" E and 0°54'38.23" - 0°53'50.23" S for Longitude and Latitude respectively. It is due to one of impacted area by the 2018 earthquake and situated within proximity to areas that experienced widespread liquefaction. Specifically, this area lies approximately 5.89 km east of Balaroa, 3.4 km west of Petobo, and 800 m east of the Palu River (Figure 2). Previous research

has classified this area as highly susceptible to liquefaction (Widyaningrum Risna, 2012) due to its geological characteristics. These include the presence of Quaternary deposits (Sukamto RAB., 1973) composed of poorly sorted gray sand with high porosity and low permeability in the southern part, and brittle, highly plastic brown to dark brown shale in the northern part (Sukamto RAB., 1973). Moreover, the other information explained that the surface condition in focused area is dominated by sand dominated weathered soil with higher than 1m thickness and shallow water table, typically found within 0.5-16m from the surface (Widyaningrum Risna, 2012).

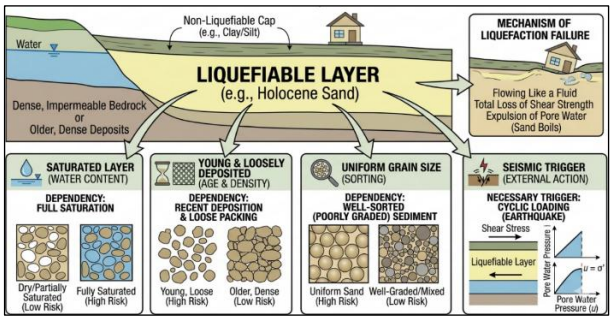

Fig. 1. Illustration of liquefaction phenomenon which is depended on several factors including saturation conditions, young and loose material, well sorted (poorly graded) sediments and triggered by seismic shaking (modified from Kramer, 1996; Tohari et al., 2011; Tuttle et al., 2019; Widyaningrum Risna, 2012 and generated by Gemini)

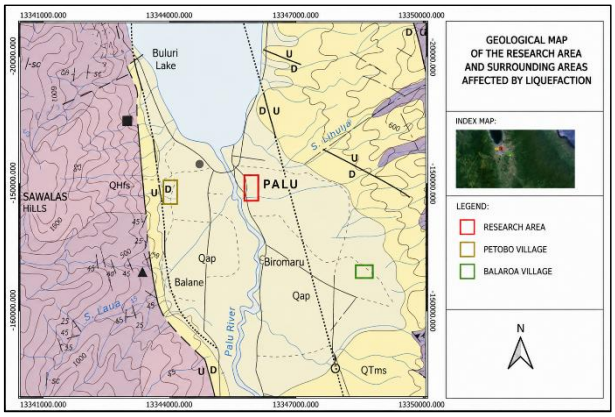

Fig. 2. Regional geological map of Palu city and study area (red rectangular) and affected, Petobo and Balaroa areas, of liquefaction in 2018 (Sukamto RAB., 1973), showing the expansive of quaternary deposit and location of Palu-Koro fault to the study area

Despite this high susceptibility, the South Palu sub-district did not experience liquefaction during the 2018 earthquake. This anomaly necessitates a detailed investigation to understand the subsurface conditions contributing to this unexpected behavior. Therefore, the employing of DC-resistivity method is necessary to provide insights into the subsurface resistivity structure, which can be correlated with lithological variations and groundwater conditions, ultimately enhancing our understanding of liquefaction potential in this area.

Direct current (DC) resistivity method is a well-known geophysics method to images geological subsurface based on electrical properties of rocks and massively successful for various application namely fault zone mapping (Yusran et al., 2020), geothermal study (Fatimah et al., 2025), aquifer identification (Musa and Murniasih, 2021) (Rizka and Satiawan Soni, 2019), geotechnical surveys (Braga et al., 1999) (Anukwu et al., 2017), including to comprehend the fluid properties at subsurface (Rizka et al., 2020) . In this study, its method was utilized because resistivity methods could provide the rapid and valuable geological information such as the shape, layer thickness and depth of the different geological units, as well as depth of the ground water table, etc). Its result will be used extensively to assess the potential for liquefaction recurrence in Palu City, following the devastating 2018 earthquake.

2. Methodology

This study employs DC-resistivity as the main method to achieve the goal of study. DC-resistivity is based on Ohm law where the resistance (R) of the object is directly proportional to the voltage (ΔV) and injected current (I) used. To obtain field resistivity data (ρ_{app}) so the direct current is necessary to be injected and simultaneously record the polarization voltage using two electrodes respectively. However, electrical resistance (R) is not the main parameter, but its properties, electrical resistance, should be normalized with the geometry of the object or known by geometrical factor (K) to obtain the apparent resistivity (ρ_{app}) data. By modified the Ohm's law and match it with the electrode configuration (i.e Wenner, Schlumberger, Dipole-dipole, etc), which is used in data acquisition, the geometrical factor is a coefficient to convert the electrical resistance (R) observed in each field observation into the electrical resistivity as seen in the following equation.

$$\Delta V = \frac{I\rho}{2\pi}\left\{\left(\frac{1}{AM}-\frac{1}{BM}\right)-\left(\frac{1}{AN}+\frac{1}{BN}\right)\right\} \quad (1)$$

$$\rho_{app} = \frac{\Delta V}{I}K^{-1} \quad (2)$$

Bi-dipole or also known as dipole-dipole configuration (figure 3) is one of the commonly used array configurations in resistivity method to acquire field resistivity data as carried out in this study at total eight lines of 2D resistivity data. The electrode spacing was fixed at 10m, while the distance between the current and potential dipoles was systematically varied from 10 – 60m. This variation in dipole separation was designed to enhance the depth of investigation, allowing resistivity data to be obtained from deeper subsurface layers. The use of multiple dipole lengths improves sensitivity to both shallow and deeper structures, thereby supporting a more comprehensive interpretation of the distribution of subsurface resistivity, which is crucial for identifying zones potentially associated with liquefaction from the deeper depth.

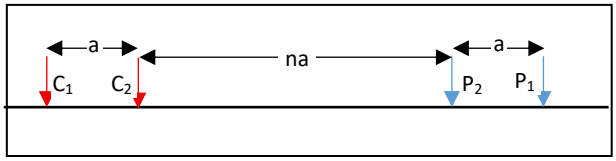

Fig. 3. Illustration of Bi-Dipole or also known as dipole-dipole configuration array for field resistivity data acquiring

The data obtained is then processed using ResIPy software with the regularized inversion algorithm. ResIPy is an open-source tool which offers an intuitive graphical user interface (GUI) particularly for handling reciprocal measurements and improving the signal to noise ratio (Blanchy et al., 2020). The results obtained from the inversion program are in the form of variations in resistivity values, depth, and layer thickness which are then analysed and interpreted. To achieve the optimum normalized inversion error (NIE) value, iteration was carried out several times in inversion process. The NIE obtained shows a convergent model where NIE is the difference between the observation and calculated data divided by the standard deviation of the observation and it is close to zero as seen on figure 5 (A. Binley et al., 1995).

In addition, once inversion process was completed and optimal NIE value is convergence (close to zero), then the 2D optimum subsurface resistivity model is obtained and ready to be analysed and interpreted (figure 6-8). The normalized inversion error is a straightforward yet critical parameter that quantifies the matches between observed field data and the calculated proposed model from inverse process. It expresses the misfit in percentage terms, enabling an objective assessment of the model reliability. Lower normalized error values, close to zero, mean an excellent fit or the model accurately represents the resistivity structure of subsurface conditions. Conversely, higher value would signify that inversion model fails to adequately reproduce the measured data, suggesting the need for further parameter adjustment or the field data measurement was classified as bad data.

3. Results & Discussion

3.1 Resistivity Model from Inverse Modeling

There are eight resistivity models which are obtained through data processing and inversion, each corresponding to the high-quality field resistivity measurement. The inversion process produced models that are considered optimal as indicated by their low value of normalized inversion error, with values approaching or close to zero as seen in figure 5. Consistently low error values were obtained across all eight models in this study reinforce the robustness of the inversion results and enhance confidence in the subsequent geological interpretation derived from these resistivity models. To get more accurate interpretation results, supporting data related to the condition of the research area are necessary, such as geological condition, rock-specific resistivity values, and previous research results around the research area.

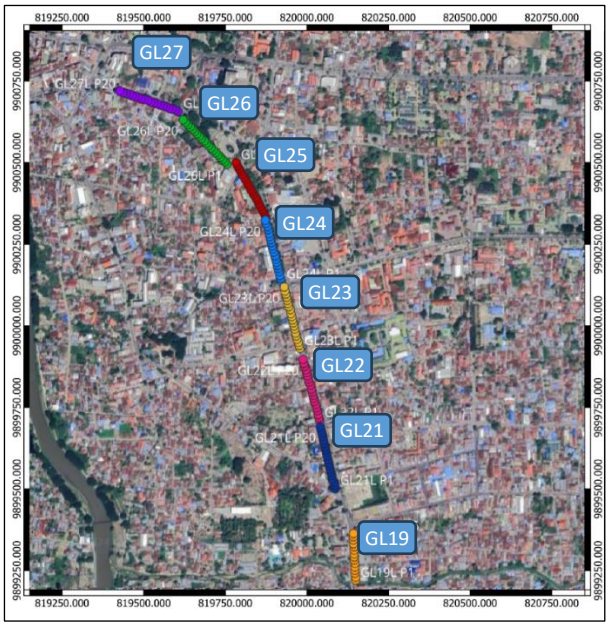

Fig. 4. The location of eight 2D resistivity lines at South Palu Sub-district, relative to eastern part of Palu River with ± 750m distance

The range of resistivity value obtained in focused study area are 4.1 – 300 ohm.m and it can image the subsurface condition up to 30m depth. The narrow range of resistivity values obtained indicates a relatively homogenous subsurface condition, particularly in term of lithology. The variations of resistivity are typically associated with changes in material properties such as mineral content, grain size, porosity and moisture content as well as degree of saturation. Once the resistivity values fall within limited range over a certain area or depth, it can be interpreted that the physical properties are relatively uniform.

Homogeneity in the subsurface implies that the geological materials present, such as clay, shale, sand, or gravel, do not vary significantly and from this results resistivity of subsurface in this area are consistently in lateral. This can be an indicative continuous lithological unit or sedimentary layer laterally. However, the noteworthy findings are once the increasing resistivity value through depth particularly around and deeper than ±11m depth. The resistivity is increasing from 53.4 ohm.m to become higher than 250 ohm.m as seen in figure 6. The increasing of resistivity vertically could be an indication of lithology changing from loose or porous layer to more compacted layer and in this study area could be interpreted as a base-soil or bedrock.

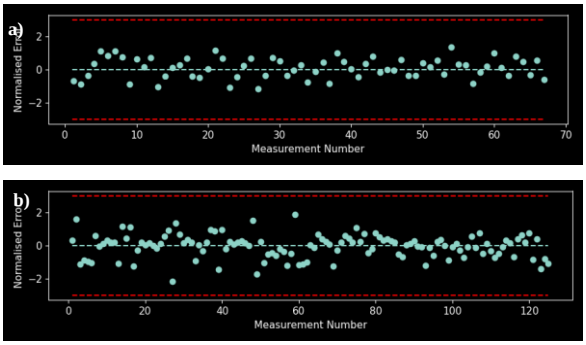

Fig. 5. The normalized inversion error of line GL19 (a) and GL 26 (b) which shows the distribution of measurement close to zero. This result can justify the model obtained are convergent (optimum) already with good quality

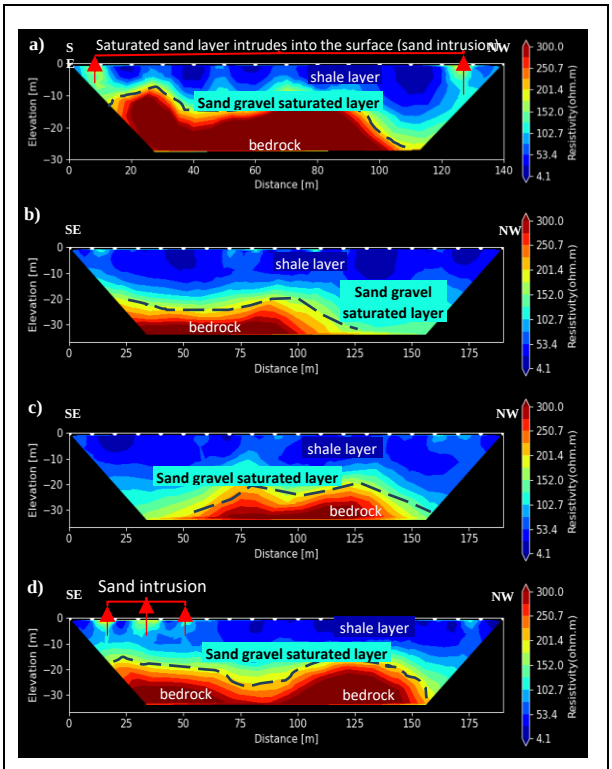

Fig. 6. Inversed resistivity model of southern part of four 2D resistivity line, Line GL19 (a), GL21(b), GL22(c) and GL23(d), show the similar pattern of resistivity distribution laterally and vertically with narrow resistivity value, 4.1 – 300 ohm.m

Different patterns of resistivity distribution were seen in two 2D resistivity lines located in the middle part of the study area, specifically in lines GL24 and GL25. These two lines show a narrower range of resistivity values compared to the others line. It indicates a more homogeneous subsurface condition as shown in figure 7. Resistivity values greater than 250 ohm·m were not identified in GL24 and GL25, unlike in other lines where high-resistivity zones appear. This homogeneity in resistivity is significant information for geotechnical analysis, as it suggests consistent subsurface material properties and reduces uncertainty in interpretation. A more uniform subsurface allows for more reliable predictions of soil behavior, particularly critical in hazard-prone areas like in this focused area study, where understanding ground conditions is essential for assessing liquefaction risk and other geohazards.

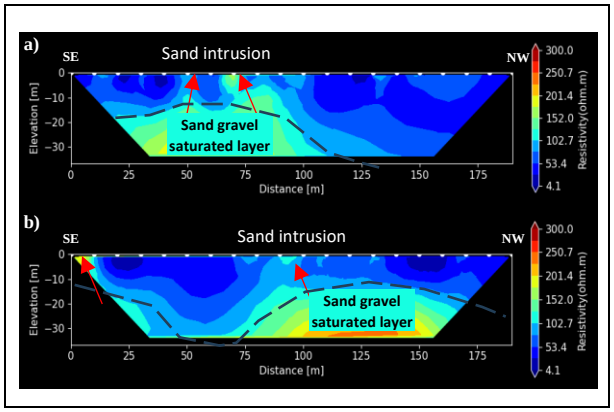

Fig. 7. Inversed resistivity model of middle part of two 2D resistivity line, Line GL24 (a) and GL25(b), which shows a narrower of resistivity value range compared to others as well as the non-appearance the high-resistivity layer (> 250 ohm.m)

The more significant different result is shown in line GL26 and GL27 which is located at northern part of the focused study area. The resistivity range value of these two-resistivity line is still the same from 4.1 – 300 ohm.m but in these two lines are found the highest resistivity value appears in the surface with 10m of thickness (white dash circle). Moreover, the resistivity distribution is not only vertically (increasing through depth) but also laterally as seen in GL26. Low-high resistivity zone appears laterally which indicates a boundary of resistivity structure which represents the geological condition.

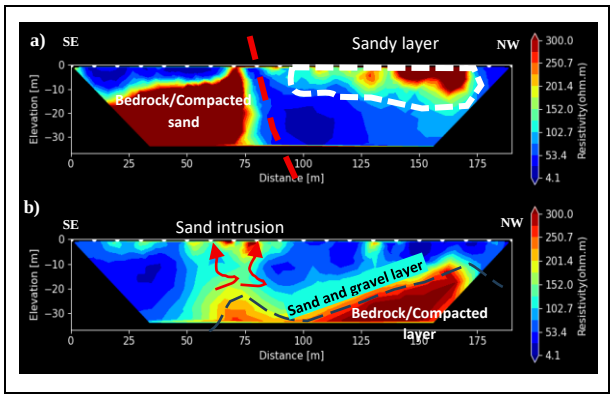

Fig. 8. Inversed resistivity model of northern part of two 2D resistivity line, Line GL26(a) and GL27(b), which shows the contrast pattern of resistivity value which indicates the boundary of formation or lithology or the existence and high resistivity layers which appear in the surface or close to the surface

In addition, analysis of the resistivity pattern and value ranges from all the resistivity models obtained indicates that the subsurface condition in this area can be classified into three (3) main layers. Layer-1 exhibits low resistivity values ranging from 4.1 – 80 ohm.m from surface to varied ±10m depth. This low resistivity values in alluvial formation could be interpreted as weathered soil (Widyaningrum Risna, 2012) and in this focused area study is interpreted as sandy shale with rich-clay layer. This layer is typically associated with fine-grained, poorly sorted with good porosity, rich-clay material with low permeability. The presence of this low permeable layer above more permeable layer (liquefiable) can play a critical point in the liquefaction process. It is due to the low permeability layer that can act as a confining cap which traps pore water pressure within the underlying sandy or gravel layer which is seen at layer-2 in this study.

Layer-2 with resistivity values between 80 – 200 ohm.m and found varied at ± 10 to 20m depth can be classified as a transition layer from compacted sandy layer with a thickness approximately 5 – 10m. This is a layer of particular interest in this study because it is composed predominantly of saturated sand and gravel, materials known for their higher permeability and lower cohesion once associated with liquefaction phenomenon. Moreover, based on resistivity value and layering resistivity structure in layer-2, this layer could also be acted as an aquifer layer in this focused area. These characteristics found in layer-2 make it the main source material for liquefaction, as such unconsolidated sediment can lose strength rapidly once subjected to seismic shaking, and act also as the aquifer layer. These features are notably seen in several resistivity cross sections where the evidence of upward intrusion (sand intrusion) of this material towards the surface was identified. These features are suggested as past or potential liquefaction events.

Layer-3 acts as the last layer that could be identified from the model, is characterized by high resistivity values exceeding 200 ohm.m and interpreted as hard soil or compacted sandy deposits. This layer also could be interpreted as the soil basement or bedrock in this focused study area. This layer is more consolidated, well-drained, and mechanically stable, offering greater resistance to deformation under stress. This layer is identified at ± 10 – 15m depth at southern part but deeper ±25 – 30m depth at middle part, line GL24 and GL25 (figure 7), and shallower at northern part, line GL26 and GL27 (figure 8).

Additionally, based on resistivity modelling results, particularly at line GL-26 at northern part of area study, was found a laterally changing as an indicative of a fault or lithology contact or boundary. It is clearly shown where the resistivity value is changed laterally from high resistivity value (> 250 ohm.m) in southern part to low resistivity value (< 53.4 ohm.m) in northern part. It's found from resistivity results could be crucial information, especially for geotechnical assessment for any further purposes.

3.2 Discussion and Geological Interpretation

The results and interpretations of each resistivity model, as discussed in the previous section, need to be transformed into geological explanation or interpretation. Moreover, those results also need to be compared with previous related studies or geophysical studies in focused areas to obtain a comprehensive understanding of liquefaction occurred in this area and or the potential of liquefaction recurrence in this study area. It is a particularly crucial step because several indicative features of previous liquefaction events are exhibited specifically at GL19 in southern part, GL23, GL24, GL25 in the central and GL27 in the northern part of focused study area. Its pattern needs to be considered since it can become a potency of liquefaction further. The pattern of liquefaction indicative features in each line has a similarity pattern to each other as

seen in figure 9 where the moderate of resistivity value, which is interpreted as the sand layer of layer-2 (transition of soft to hard layer), intruded a top layer which is interpreted as weathered soil composed by sandy shale with rich-clay dominant. Some sand intrusion features are imaged well from the subsurface to surface as seen in fig 8 at line GL26 however the other features stop at certain depth (not until the surface), it is obviously seen in middle to southern part of this study area. The increasing of resistivity value generally shown in all resistivity lines which is in accordance with the subsurface geological conditions in western parts of the Palu city which is consisted of moderate resistivity layers (< 300 ohm.m) and represents the alluvial fan in this area (Marjiyono et al., 2013).

One of the most compelling pieces for liquefaction evidence is the occurrence of sand intrusion or known also as sand volcano or sand blow, a subsurface to surface migration of sand and other loose materials through cracks or fractures caused by elevated pore water pressures during seismic shaking. These intrusions typically form dikes or vents that fill with sand and leave a distinct signature even in surface or subsurface as seen from figure 6 – 8. In the resistivity models obtained, such upward intrusion features, sand intrusion, or also known as sand blow or sand volcano (figure 10) are represented by moderate resistivity values in the range of 78.6-200 ohm.m, extending from depth toward the surface. Range of these resistivity values is closely the same with 2nd resistivity layer which is interpreted as part of saturated sand gravel layers. This feature is consistent with saturated sandy or gravel material which are electrically more conductive than dry and compacted soil but more resistive than clay-rich sediments. The similarity in the resistivity patterns shown across the identified lines suggests that these features correspond to sand intrusion, direct products of liquefaction. Moreover, the continuity of sand intrusion features are also seen a fence diagram as shown in figure 9 (red arrow), where the sand intrusion in northern part is quietly massive, wide and up to the surface whilst in middle part the sand intrusion features are stopped in a certain depth as well in southern part the features is such less than in the northern part. Thereby, these found are reinforcing the interpretation of post or potential liquefaction prone zones within study areas particularly in middle to southern parts which have a recurrence potency of liquefaction.

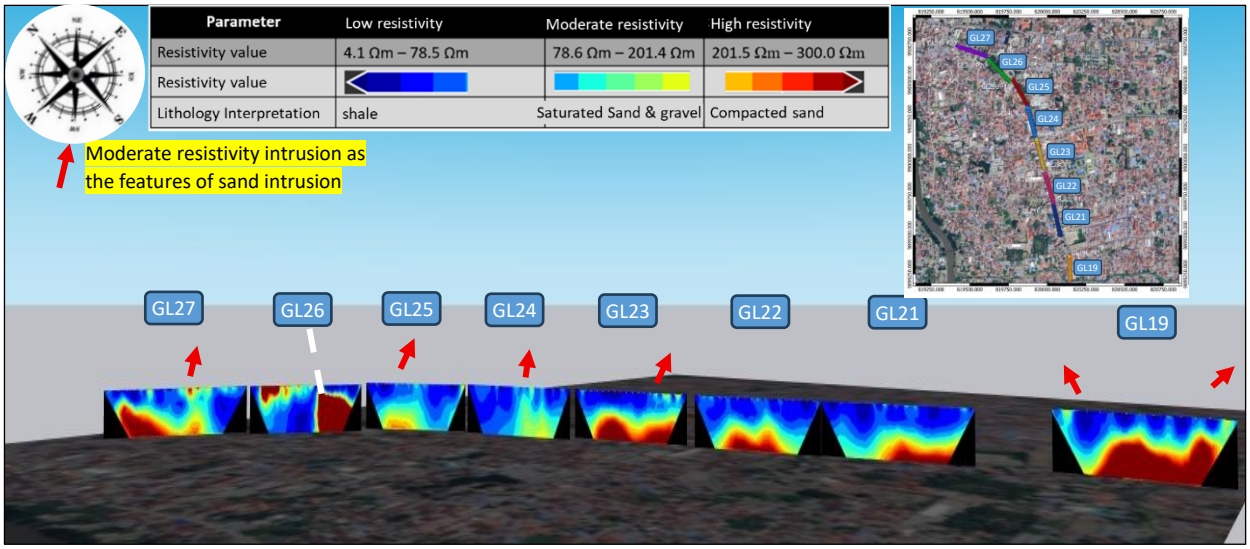

Fig. 9. Visualization of all resistivity models from eight resistivity lines in fence diagram which show the correlation of resistivity structure laterally and vertically in focused study area. Moreover, it also shows the upward of moderate resistivity intrusion (red arrow) at several lines in south, middle and northern part of study area

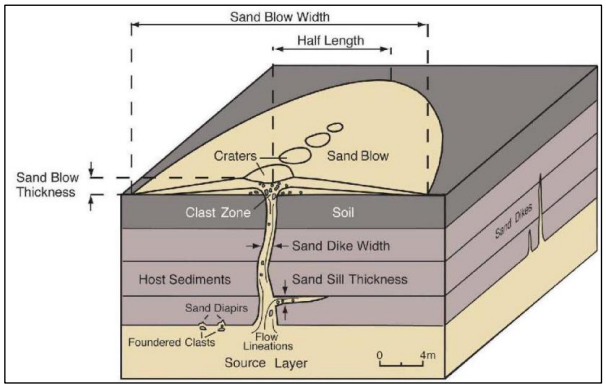

Fig. 10. An illustration of sand intrusion, one product of liquefaction where the saturated sand or loose layer from a certain depth intrudes to the surface and form a dyke or vent signature (Tuttle et al., 2019)

4. Conclusion

The resistivity measurement and analysis successfully delineate the subsurface characteristics of the study area up to a depth of approximately 30m. The model obtained from inversion process, characterized by low normalized inversion errors, indicates high model reliability and good data quality. The resistivity range of 4.1 – 300 ohm.m suggest a relatively homogeneous subsurface dominated by fine – medium grained sediments typical of alluvial fan deposits. Three main layers were identified consisting of,

a. Layer-1 (41. – 80 ohm.m) which is interpretated as sandy shale or clay-rich soil with low permeability, acting as a confining layer.
b. Layer-2 (20 – 200 ohm.m) which is interpreted as saturated sand and gravel, representing both an aquifer zone and the most potential liquefiable layer.
c. Layer 3 (>200 ohm.m) which is interpreted as compacted sand or hard soil acting as the subsurface soil basement.

Several indicative features of liquefaction, such as upward-moderate resistivity intrusions interpreted as sand blows or sand dikes, were identified in several resistivity lines (GL-19, 23 and GL-27). These features are consistent with post – or potential liquefaction processes. However, despite the presence of these indicative features, there is no substantial field evidence that large scale liquefaction occurred during the 2018 Palu earthquake.

This finding suggests that the existence of potentially liquefiable layers as revealed by resistivity models does not directly correspond to the actual occurrence of liquefaction. The manifestation of liquefaction depends on multiple factors such as seismic intensity, groundwater level, soil compaction, and permeability contrast between layers as well. Localized small-scale liquefaction may have occurred but without significant surface deformation.

Overall, the results indicate that the study area still possesses potential for future (recurren) liquefaction, particularly if subjected to strong seismic shaking or changes in hydrogeological conditions. Continuous geophysical monitoring and the integration of resistivity data with geotechnical and seismic assessments are essential for improving the accuracy of liquefaction hazard mapping and for mitigating risk in future infrastructure development.

Acknowledgements

We would like to thank PT. Abhinaya Mappindo Bumitala for the access and permission to use the resistivity data set for this study.

References

A. Binley, A. Ramirez, & W. Daily. (1995). Binley_et_al_1995. In M.S. Beck (Ed.), The 4th Workshop of The European Concerted Action on Process Tomography (Number 1995, pp. 401–410).

Anggorowati, V. D. A., & Qodri, M. F. (2026). Soil Behavior and Liquefaction Potential During Earthquake in Kulonprogo, Yogyakarta, Indonesia. Journal of Geoscience, Engineering, Environment, and Technology, 11(1), 95–100.

Anukwu, G. C., Adebara, A. F., Abodunrin, T. K., & Iwakun, A. P. (2017). Soil Structure Evaluation Across Geologic Transition Zones Using 2D Electrical Resistivity Imaging Technique. Journal of Geoscience, Engineering, Environment, and Technology, 2(2), 95–101.

Bastola, A., & Acharya, I. P. (2016). Liquefaction Susceptibility Mapping of Kathmandu Valley. Proceeding of IOE Graduate Conference, 19–25.

Blanchy, G., Saneiyan, S., Boyd, J., McLachlan, P., & Binley, A. (2020). ResIPy, an intuitive open source software for complex geoelectrical inversion/modeling. Computers & Geosciences, 137, 104423. https://doi.org/https://doi.org/10.1016/j.cageo.2020.104423

Braga, A. C. O., Malagutti F°_, W., Dourado, J. C., & Chang, H. K. (1999). Correlation of Electrical Resistivity and Induced Polarization Data with Geotechnical Survey Standard Penetration Test Measurements. Journal of Environmental and Engineering Geophysics, 4(2), 123–130. https://doi.org/10.4133/JEEG4.2.123

Fatimah, Trisnaning, P. T., & Trianda, O. (2025). Geothermal Potential of the Dimanjar District, Sumberarum,Tempuran Area Using Resistivity and Geochemical Data Approaches. Journal of Geoscience, Engineering, Environment, and Technology , 10(1), 59–63.

Ishihara, K., Yasuda, S., & Yoshida, Y. (1990). Liquefaction-Induced Flow Failure of Embankments and Residual Strength of Silty Sands. Soil and Foundations, 30(3), 69–80.

Kramer, S. L. (1996). Geotechnical Earthquake Engineering (1st ed.). Prentice Hall.

Kuswandi, Y., Erwindi, J., Hadian, M. S. D., & Muslim Dicky. (2020). Disaster Mitigation for Palu City residents in Dealing with Liquefaction Disasters in Accordance of Spatial Patterns of Palu City, Central Sulawesi Province, Indonesia. Journal of Geoscience Engineering, Environment, and Technology, 05(4), 191–197.

Marjiyono, H. Kusumawardhani, & A. Soehaimi. (2013). Struktur Geologi Bawah Permukaan Dangkal Berdasarkan Interpretasi Data Geolistrik, Studi Kasus Sesar Palu Koro. Jurnal Sumber Daya Geologi, 23(1), 39–45. https://jgsm.geologi.esdm.go.id/index.php/JGSM/article/view/98

Musa, M. D. Th., & Murniasih, S. (2021). Identifikasi Lapisan Akuifer di Kelurahan Petobo Kota Palu Menggunakan Metode Geolistrik Hambatan Jenis. Gravitasi, 20(2), 34–41. https://doi.org/10.22487/gravitasi.v20i2.15531

Rizka, R., Piskora, B. A., Satiawan, S., & Saputra, H. (2020). Simulation of Time-Lapse Resistivity Method on Sandbox Model to Determine Fluid Changes and Desaturation. Journal of Geoscience, Engineering, Environment, and Technology, 5(4), 227–233. https://doi.org/10.25299/jgeet.2020.5.4.4266

Rizka, & Satiawan Soni. (2019). Investigasi Lapisan Akuifer Berdasarkan Data Vertical Electrical Sounding (VES) dan Data Electrical Logging; Studi Kasus Kampus Itera. Bulletin of Scientific Contribution: GEOLOGY, 2(17), 91–100.

Soehaimi, Sopyan Yayan, & Sulistyawan Ibnu Hajar. (2018). Genetika Gempabumi. In DiBalikPesonaPalu (1st ed., pp. 33–40). Badan Geologi.

Soehaimi, Sopyan Yayan, & Sulistyawan Isnu Hajar. (2018). Seismotektonik Palu dan Sekitarnya. In Di Balik Pesona Palu (1st ed., pp. 21–32). Badan Geologi.

Sukamto RAB. (1973). Peta Geologi Tinjau Lembar Palu, Sulawesi (2nd ed.). Pusat Penelitian dan Pengembangan Geologi.

Tohari, A., Sugianti, K., & Soebowo, E. (2011). Liquefaction Potential At Padang City: Comparison Of Predicted And Observed Liquefactions During The 2009 Padang Earthquake. Jurnal RISET Geologi Dan Pertambangan, 21(1), 7. https://doi.org/10.14203/risetgeotam2011.v21.42

Tuttle, M. P., Hartleb, R., Wolf, L., & Mayne, P. W. (2019). Paleoliquefaction Studies and the Evaluation of Seismic Hazard. Geosciences, 9(7). https://doi.org/10.3390/geosciences9070311

Widyaningrum Risna. (2012). Penyelidikan Geologi Teknik Potensi Liquifaksi Daerah Palu, Provinsi Sulawesi Tengah. http://www.dgtl.dpe.go.id

Yusran, M., Massinai, M. A., & Syahruddin, M. H. (2020). Studi Zona Sesar Menggunakan Metode Geolistrik Resistivitas dan Data Geologi Permukaan di Kecamatan Ujungloe Kabupaten Bulukumba. JURNAL GEOCELEBES, 4(1), 53–60. https://doi.org/10.20956/geocelebes.v4i1.9233